

Harmonizing Blasting Efficiency: A Case Study on Evaluation and Optimization of Fragmentation Size and Ground Vibration

M. Naresh¹ · N. Sri Chandrahas¹  · G. Praful Kumar² · T. Pradeep Kumar¹ · K. Sravan Kumar¹

Received: 20 January 2024 / Accepted: 1 April 2024
© The Institution of Engineers (India) 2024

Abstract Drilling and blasting techniques persist as the most economically viable approaches for rock excavation in both surface and underground mining. However, the conventional focus has predominantly centered on optimizing rock fragmentation, often overlooking the consequential impacts of by-products, such as ground vibration and fly rock. The core objective, which is not entirely met by the current utilization of explosive energy for rock mass breakage, reveals that a mere 20–30% of the explosive energy effectively contributes to shattering the rock mass. The remaining percentage is dissipated as ground vibration, air blast, noise, fly rock, back breaks, and other ancillary effects. This investigative endeavor involved a comprehensive examination of an operational mine, incorporating a series of blast exercises to systematically evaluate the impact of various blast design parameters, including burden, spacing, stemming length, bench height, powder factor, explosive quantity, and maximum charge/delay. For the interpretation and analysis of results, sophisticated software and instrument such as Wipfrag and Minimate Plus seismograph were employed. The unveiled findings indicate that specific blast design parameters, such as a burden of 4 m, spacing of 5 m, stemming length of 5 m, bench height of 6 m, powder factor of 2.25 te/kg, and maximum charge/delay between 55 and 60 kg, were instrumental in yielding favorable blasting outcomes. These parameters led to mean fragmentation sizes below 100 mm and peak particle velocities below 10 mm/s, thereby

highlighting the potential for enhanced efficiency in rock excavation through meticulous blast design considerations.

Keywords Mean fragment size · Peak particle velocity · WipFrag and Minimatepl

Introduction

Mineral resources form the backbone of industry and non-metals and metals are needed as fundamental materials. Both underground and open pit mining methods are used to recover mineral resources. Mineral extraction is achieved in both cases by loosening coal and rock. Open pit mining is the most popular form of mineral extraction in the world. The mineral extraction process begins with the drilling and blasting operation. The basic goal of blasting is to break rock and move broken rock. Communities may be subject to excessive noise and vibration as a result of blasting operations. Ground vibration from blasting can produce excessive structural vibration, which can cause damage. Dams, buildings, well slopes and roads can be severely damaged by ground vibration [1, 2]. As a result of having accurate ground vibration prediction, you can help limit the environmental effects of blasting. The intensity of ground vibration is determined by a number of variables that can be divided into two categories: controllable and uncontrollable variables. Most of the control parameters are associated with explosive criteria (initiation system, initiation sequence, number of free faces, stops, explosive energy, loading geometry, loading method) and blast hole design parameters (depth of hole, diameter of hole, sub drill depth, inclination of hole, neck height, bucking, pattern blast, load to spacing ratio, blast area and configuration, blast size and configuration and blast, initiation direction, boot system.

✉ N. Sri Chandrahas
srichandru2009@gmail.com

¹ Department of Mining Engineering, Malla Reddy Engineering College, Hyderabad, India

² Department of Mining Engineering, Indian Institute of Technology, Dhanbad 826004, India

The degree of ground vibration is determined by a number of factors. These variables fall into three categories: blast design parameters, explosive parameters, and rock mass properties. Blasting engineers can adjust blast design parameters or controllable factors, including loading, spacing, drift, drilling secondary, the type of explosive material, the maximum weight of charge used per delay. (W), diameter and depth of the hole and specific load [3, 4]. The second group includes the type of explosive (ANFO, gel water, emulsion or dynamite, SME), as well as the detonation velocity (VOD), density and powder factor (kg ANFO/m³). These categories of factors can also be controlled. Blasting engineers cannot affect rock mass characteristics or uncontrolled parameters, such as rock compressive strength in the third group [5]. The selection of diameter depends on several factors such as desired degree of fragmentation, rock mass characteristics, size of operation type of explosive used and cost factor [6]. Similarly, Both rock fragmentation and ground movement are greatly influenced by blast design characteristics such as spacing load ratio, firing pattern, and explosive quantity [7]. The diameter be kept between 0.5 and 1.25% of the bench height. Whenever large block rock is uncounted it is suggested that the smaller diameter holes be used [8].

To estimate blast parameters and determine the amount of explosives to use to prevent blocking or allow good fragmentation, all of these factors require careful research and field testing [9]. Likewise, Rai and Yang illustrated some significant fragmentation concerns observed during rounds of blasting in limestone quarries. In order to properly manage concerns in field-sized blast rounds, the study looked at the impact of some key design criteria on blast performance [10]. The current rock fragmentation technique in mining in India needs to be re-examined in order to increase mine productivity. It is critical that we gain a better understanding of the explosive utilized and the rock mass that will be blasted. Traditional blasting methods such as Powder Factor (cubic meter of rock broken per kilogram me of explosive), identifying the target rock as weak, medium, or strong, or specifying a delay interval in multi-hole blasting cannot yield enhanced productivity [7]. A firing pattern gives the explosive charges a coordinated chance to use their combined effect. As a result, the firing pattern offers a clear

view of the following blast holes in some order as the blast evolution progresses. The firing pattern controls the throw's motion and trajectory. The firing pattern shows a significant impact on the twin blasting by-products of fragmentation and ground vibration. It was discovered during the blast trials that the V pattern fragmented more effectively, likely as a result of in-flight contact between fractured rock fragments [7]. Similar to this, tests revealed that ground vibration and fragmentation results can both be considerably influenced and governed by firing patterns [11].

Rock Fragmentation

Explosive detonation releases a huge amount of energy in the form of gas and heat. The explosive gas pressurizes the borehole and creates radial compressive stress that is significant enough to begin and spread fractures under high pressure. Gas enters and expands the principal radial cracks and spontaneous cracks [12]. The rock mass will yield and be hurled forward if the distance between the free face & the blast hole is calculated appropriately. Fragmentation achieved after the blast occurred is a significant parameter for determining optimal blasting. In most situations, vibration and fragmentation are linked, with poor rock fragmentation correlating to increased vibration detection. Proper fragmentation is critical to the mine's overall profitability [13].

Size Distribution

The size of the fragmentation depends on a variety of mining parameters, including the size of the loading and hauling equipment, the processing setup, and the general layout of material handling and transport. Some of the sizes associated with fragmentation study are included in Table 1 below [14–18].

Mean Fragmentation Size

Large-scale fragmentation measurement is a difficult issue, and substantial study has been conducted using various methodologies and technologies for fragmentation assessment. Some of the traditional, laborious, and time-consuming ways of assessing fragmentation include sieving or screening, the oversize

Table 1 Some of the size designation of the blasted fragments and their meanings

D_n	The equivalent spherical diameter or nominal diameter, i.e., the diameter (m) of a sphere having the same volume as that of the fragment
D_{10}	D_{10} indicates that 10% of the sample by weight is finer and the remaining are courser. The same goes for D_{20} , D_{80} there 20% and 80% of samples are finer, and the remaining are courser
D_{50}	It is the median value of D_n , for which half of the sample is finer and half courser
D_{10}	D_{10} Indicates that 10% of the sample by weight is finer and the remaining are courser
D_{20}	The same goes for D_{20} ,
D_{80}	D_{80} there 20% and 80% of samples are finer, and the remaining are courser

boulder count method, and the shovel loading rate method [19]. Methodologies used in current procedures include visual analysis, photogrammetry, and image analysis. Many of these measuring techniques are employed by the mining industry and researchers; however, most of them are time-consuming, inconvenient, and inaccurate. Aside from the approaches stated above, other empirical models have been offered in the literature, including the Kuz-Ram model, Larsson's equation, Sve-DeFo formula, and others. For fragmentation, various image processing method shows good results and analyses fragmentation effectively. Some of them are: WipFrag, FRAGSCAN, ImageJ, etc. In these methods, post-processing of images takes place [20–22].

Induced Ground Vibration

Vibrations move in two directions during blasting operations. A useful ground wave measuring criteria are to record the vibration's main frequency and peak particle velocity (PPV). Overpressure can be measured by measuring the sound pressure intensity in decibels (dB). Much research has shown a relationship between the PPV of ground vibration and the distance and maximum charge per delay (Q) [16]. The United States Bureau of Mines (USBM) provides one of the most prominent and often used equations for linking PPV to distance and Q, which is presented in Eq. (1). Scale distance is shown as a function of radial distance and square root of maximum charge per delay in the Predictor equation.

$$PPV = k \left(\frac{R}{\sqrt{Q_{max}}} \right)^{-b} \tag{1}$$

where, PPV is peak particle velocity (m/s), k and b are site constants, Q_{max} is the maximum charge weight per delay (kg), and R is the radial distance from blasting face to point of vibration monitoring (m).

Materials and Methods

Study Area

Mine A is chosen for the research work. Mine A is in the Dholnara region of Chhattisgarh's Raigarh district and is a fully mechanized opencast mine that uses a shovel-dumper combination style of operation. The mine, which covers an area of 6.39 km², is bordered on all sides by hill ranges and forest reserves, and it shares a boundary with two other mines. A high-tension power wire runs along the mining area's northern limit. The coal belt of Mand-Raigarh coalfield extends over an area of about 3700 sq.km and constitutes almost the central part of the Son-Mahanadi Basin lies between Hasdeo-Arand coalfield in the northwest separated by a basement high and IB River coalfield in the southeast. Mines geological plan and captured photographs shown in Fig. 1 a–c.

Methodology

As illustrated in Fig. 2, the study involved the execution of trial blasts and systematic data collection. A series of blasts was conducted, considering the dynamic interplay with the prevailing geo-mechanical conditions. This iterative process continued until satisfactory outcomes were achieved in terms of both mean fragmentation size and peak particle velocity.

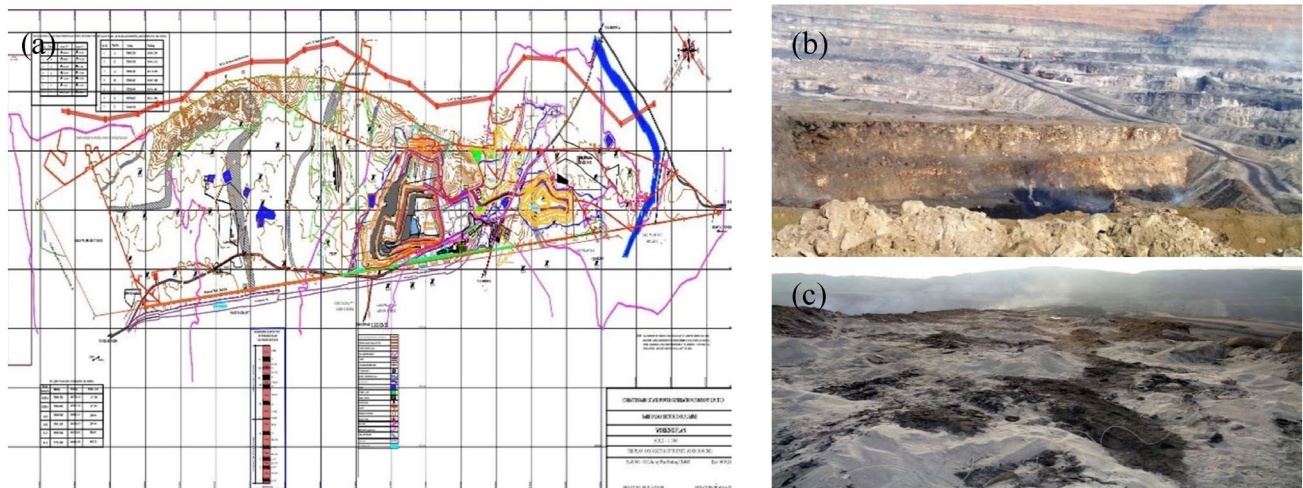
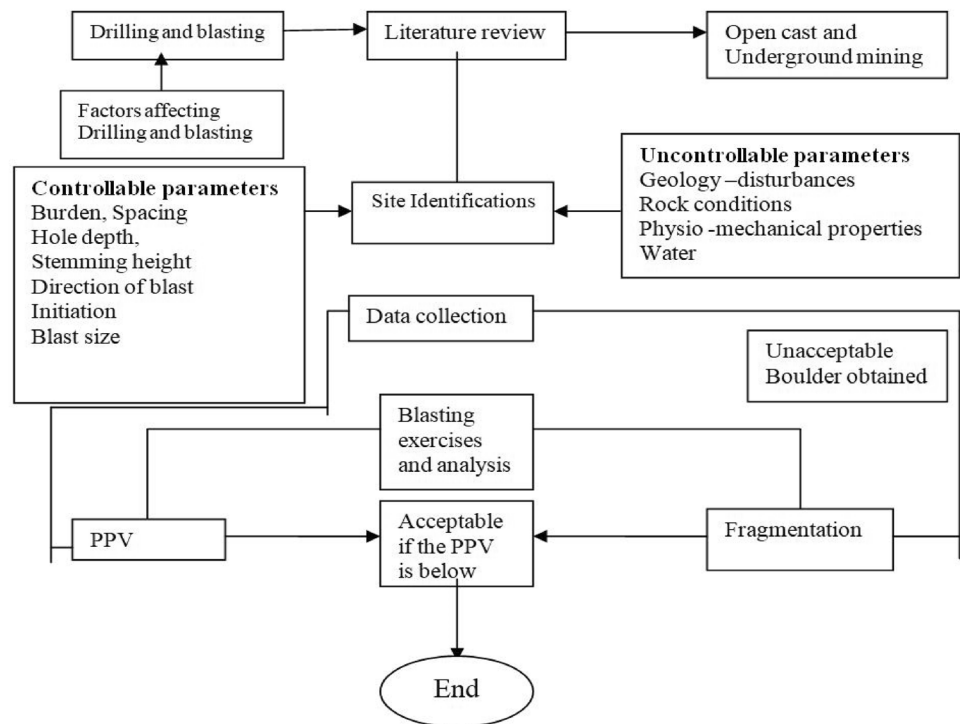


Fig. 1 a Mine plan. b, c mine and explosive charging

Fig. 2 Flowchart of the methodology followed



Data Collection

Data for this research work were collected from an opencast mine located in the Raigarh district of Chhattisgarh. Rock fragmentation immediate to the blast was captured using suitable handheld camera with appropriate pixel and resolution. Likewise, Peak particle velocity data were collected using Minimate plus in three directions. The research carried in two phases, initially in Phase I, base line data like burden, spacing, charge quantity, stemming, drilling pattern, firing pattern was collected to understand the trend and impact on rock fragmentation and peak particle velocity, data presented in Table 2 and in Fig. 3 as well.

The mine includes a core active pit, with mining operations advancing westward, and two major Overburden dumps on the eastern side of the pit. At the time of the research, blasting was taking place on the 8th seam de-coaled region, the 9th seam 1st exposure bench, as well as the Southwest and Northwest OB benches. For blasting, diagonal blasting with a staggered pattern was followed. SME was used as explosive. Tables 2 and 3 show the baseline and optimized data collected.

Principle Component Analysis

The principal component analysis method was used to identify the relation of rock mass properties to rock mass blastability [23]. Extracted component matrix of PCA described the behavior of geo-mechanical rock mass during charging

operations. Similarly, PCA worked out to find the influence of drill design, explosive and geological parameters on the swelling factor. Research unfolds; PCA is capable of identifying the relation between blast design parameters and blast [24].

PCA in XLSTAT has been used to identify the impact of design-related parameters on mean fragmentation size and the peak particle velocity [23]. The main novelty of the present study is to apply the principal component analysis (PCA) to find the effective parameters for rock fragmentation. PCA was rarely used to find the influence of blast design parameters on blasting results [24].

PCA in XLSTAT generates a correlation circle, and it is these values that guide the interpretation process. To understand the link between independent and dependent variables, XLSTAT's correlation circle is a must-have. The analysis is divided into three parts: positively correlated, negatively correlated, and orthogonally correlated. Each of these segments is examined separately. There is a positive correlation between closely spaced variables, a negative correlation between variables in opposing quadrants, and an orthogonal relationship between variables in adjacent quadrants. An orthogonal correlation suggests that there is no association between the variables at all as shown in Fig. 4.

In Fig. 4, it is evident that Explosive charge, Delay per hole, and Powder factor exhibit a positive relationship with MFS, as they lie within the same quadrant. Conversely, Cast booster, total explosive quantity, stemming length, and spacing burden ratio reveal a negative relationship, as they fall

Table 2 Blast base line data

Blasting Parameters\blast	Input data										
	Blast-1 8th Seam	Blast-2 8th Seam	Blast-3 2nd Seam	Blast-4 8th Seam	Blast-5 Top OB bench North west	Blast-6 9th seam 1st Exposure	Blast-7 Blast-7	Blast-8 8th seam de-coaled North	Blast-9 9th seam 1st Exposure	Blast-10 9th seam 1st Exposure	Blast-11
Explosive type	SME										
Blasting pattern	Staggered										
Blasting connection	Diagonal										
No. of holes	130	123	218	158	166	30	30	30	30	15	15
Hole diameter (mm)	159	160	110	158	110	110	110	110	110	110	110
Hole depth (m)	6	6	6	6	4	5.5	5	6	6	4.5	5
Bench (H) m	6	6	6	6	6	6	6	6	6	6	6
Delay per hole (ms)	250	250	250	250	250	250	250	250	250	250	250
Burden (m)	4	4	3	4	4	2.5	2.5	2.5	2.5	2.5	2.5
Spacing (m)	5	5	4	5	4	3	3	3	3	3	3
DTH (down hole)	780	738	1308	948	996	780	738	1308	948	996	950
TLD (M)	650	615	1090	790	830	650	615	1090	790	830	670
No of (ED)	1	1	1	1	1	1	1	1	1	1	1
Stemming (m)	2.2	2.2	3	3.5	2.23	2.9	2.6	3.2	3.2	3.5	3.2
Powder factor (kg/m ³)	2.24	2.24	1.75	2.14	3.3	2.24	2.24	1.75	2.14	3.3	3.2
Charge/hole (kg)	54	54	40.91	55	18.73	30	30	36	36	10	15
Explosive (kg)	7020	6642	8918.38	8690	3109.18	900	900	1080	1080	150	225

Table 2 (continued)

Blasting Parameters\blast	Input data										
	Blast-1 8th Seam	Blast-2 8th Seam	Blast-3 2nd Seam	Blast-4 8th Seam	Blast-5 Top OB bench North west	Blast-6 9th seam 1st Exposure	Blast-7 9th seam 1st Exposure	Blast-8 8th seam de-coated North	Blast-9 9th seam de-coated North	Blast-10 9th seam 1st Exposure	Blast-11
Cast Booster (kg)	13	12.3	21.8	15.8	16.6	3	3	3	3	1.5	1.5
Total Explosive (kg)	7033	6654.3	8940.18	8705.8	3125.78	903	903	1083	1083	151.5	226.5
Total volume blasted rock (m ³)	15,600	14,760	15,696	18,960	10,624	1350	1350	1350	1350	675	675

into the opposite quadrant relative to MFS. There appears to be no discernible relationship with the variables No of holes, Firing pattern, bench height, No of rows, and total broken rock, as they are orthogonal to MFS.

In the context of PPV, Cast booster, total explosive quantity, stemming length, and spacing burden ratio appear to exhibit a positive relationship, while Explosive charge, Delay per hole, and Powder factor demonstrate a negative relationship. Conversely, there seems to be no apparent relationship with the variables No of holes, Firing pattern, bench height, No of rows, and total broken rock, as they appear orthogonal to PPV.

This sensitive analysis proved instrumental in designing blasts and conducting field experiments, leading to further insights into blast results.

Trail Blasts Experimentation and Results

In this investigation, a rotary drilling machine with a 150 mm carbide bit was employed to uniformly all of the holes. ZT 44 KOMATSU DTH is typically used for all blasting with a hole diameter of 150 mm. As can be seen in picture 4.7, all of the blast holes were drilled to the appropriate depth according to the geospatial conditions that were taken into consideration. Optimal care and attention were maintained to attain precision throughout all of the blasts Down-hole delays of 425 and 450 ms were commonly chosen, with hole-to-hole delays of 17 ms and row-to-row delays of 25 and 42 ms adopted, respectively, according to rock conditions. Site Mixed Emulsion (SME) explosives were utilized for all of the trial explosions at Mine A, the initial density was maintained in the range of 1.25 g/cc to 1.29 g/cc, and the final density was obtained at 1.05 g/cc to 1.1 g/cc after a gassing time of 20–25 min.

Fragmentation Analysis

Rock fragmentation images of 11 blasts were collected after each blast and were fed into WipFrag. WipFrag analyzed an image by the scale provided on the image. Then, it divided all those rock fragments into different sizes based on the scale and produced a size distribution of each image. Then, various images of a blast were analyzed, and an average of all distributions was chosen for the size distribution of a blast. Similarly, the process was repeated for each image within each blast. Finally, the size distribution of each blast was obtained and stored in an excel sheet for further analysis.

Fragmentation monitoring was done by taking pictures of the post blasting fragmented material and performing digital image analysis to identify and relate the sizes of different fragments, and their size fractions as shown in Fig. 5a–c. Multiple fragmentation images were recorded for

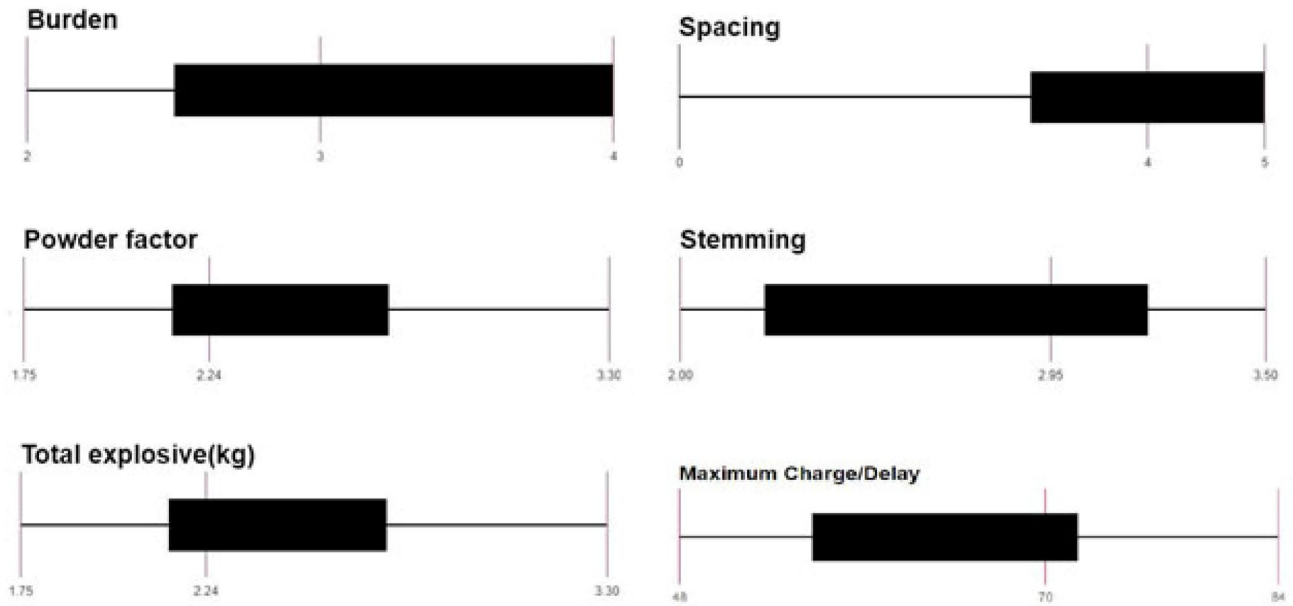


Fig. 3 Boxplot of various blast design parameters

Table 3 Distance, Peak Particle Velocity, and locations and fragmentation size

blast no	Blast location	Monitoring location	Distance from blast site (m)	PPV (mm/s)			Fragmentation size(mm)				
				X	Y	Z	D01	D20	D50	D80	D99
1	8th Seam	Viewpoint	322				31	96	22	566	968
	De-coaled Area	Viewpoint	350	1.81	2.73	4.38					
2	8th Seam	Viewpoint	322	2.67	2.54	5.71	11.9	32.8	55.6	06	324
	De-coaled Area	Viewpoint	350	2.05	3.02	3.92					
3	2nd OB Bench	Near Basti	326	5.46	3.94	2.54	12.1	33.4	56.9	109	324
	Southwest	Near Basti	289	5.56	3.86	4.10					
4	8th Seam	Near HT Line	170	8.76	5.53	6.86	12.4	33.4	56.6	108.19	325.7
	De-coaled area	Near HT	248	6.43	4.38	5.94					
5	Top OB bench	Near HT Line	170	8.89	7.37	8.80	12.23	33.43	56.16	107.17	324.06
	Northwest	Near HT Line	248	6.43	4.37	6.33	12.23	33.43	56.16	107.18	324.06
6	9th seam 1st Exposure	Near HT Line	96	4.13	11.47	10.54	15.31	53.17	113.6	228.65	464.63
7	9th seam 1st Exposure	Near HT Line	86	7.448	18.54	16.63	12.62	34.20	57.34	108.45	336.56
8	8th seam de-coaled North	Near HT Line	81	35.83	29.56	27.99	11.97	32.80	55.55	106.76	324.11
9	8th seam de-coaled North	89	21.1	19.58	23.55	21.41	12.10	33.40	56.69	109.31	314.52
10	9th seam 1st Exposure	92	10	8.5	14.55	11.0	12.23	33.47	56.63	108.8	325.6
11	9th seam	100	11.56	10.1	9.92	10.5	12.3	33.47	56.53	108.8	325.6

each blasting after a few sets of mucking operations in order to ensure representative analysis is obtained for fragmentations. The readings obtained from image analysis were scaled using known length measuring scale in the image as reference. The size fraction distribution curves were correspondingly plotted to judge the various size fractions. Digital image analysis software such as WipFrag was used for obtaining and plotting the size fractions. Total 11 blasts were conducted at field in minimal interval; results were presented

in Table 3. Similarly, Various Particle sizes produced during blasting shown in Fig. 7.

PPV Measurement

During each blast, six readings of PPV and two readings of overpressure were recorded at the two observation points. The waveforms obtained during each blast were also recorded and later processed to identify the dominant

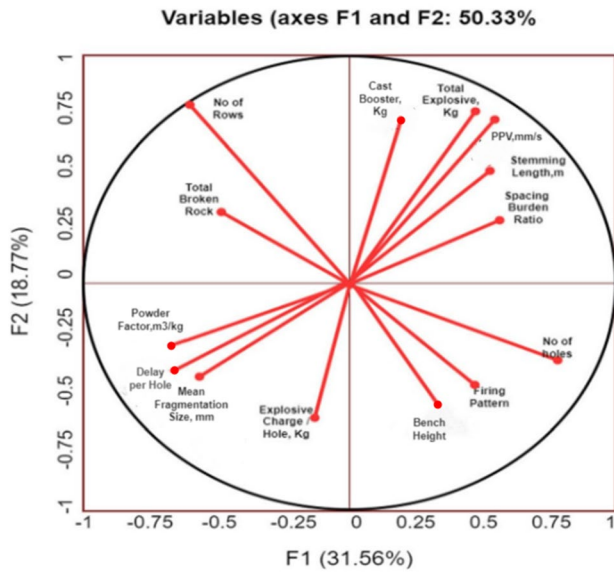


Fig. 4 MFS and PPV Correlation Circle Diagram

frequency of vibration. The readings of these vibration readings are summarized and reported in the observations section.

The ground vibration of 11 blasts was recorded at the blast site using Micromate and Micromate plus as shown in

Fig. 5d, e. After the blast, vibration data were fed into the computer from the instruments. Using that data, an FFT report and an event report of all 11 blasts were obtained in Blast ware software. Once all the data were collected, it was entered into an excel spreadsheet for further analysis. The vibration waveforms recorded after each blast was processed for identifying dominant frequency using Blast wave software. The dominant frequency is responsible for the identification of the allowed ranges of PPVs as per the DGMS guidelines. A sample identification mechanism is presented in Fig. 6.

Wave form report identified the dominant frequency obtained on each axis of geophone with associated PPV for that event (Figs. 7, 8). A summary of the event report was also generated for each blast. PPV generated from various directions such as radial, transverse and radial directions were presented in Fig. 9.

The vibration readings for six number of trial blasts conducted for assessment of vibrations within 100 m of blasting face. The distance of observation for all the trial blasts was kept between 80 and 100 m. The purpose of these blasts was to assess the level of vibration below 100 m distance and to optimize the blasting parameters in such case to keep the vibration levels within the DGMS guidelines. Blast Ware Software was used to extract FFT reports, event reports, and PPV from Minimateplus and Micromate instruments.

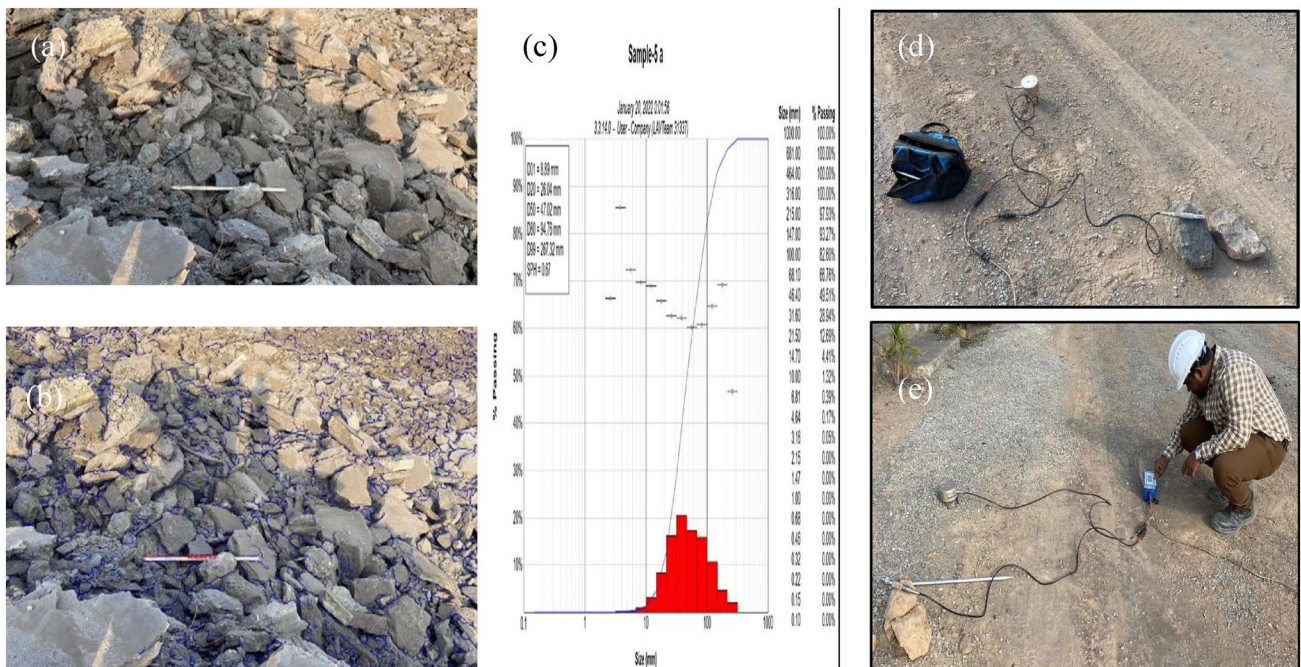


Fig. 5 a, b Image analysis of fragmented rock using the WipFrag c representative size distribution during the fragmentation analysis d, e geophone and Microphone setup in field

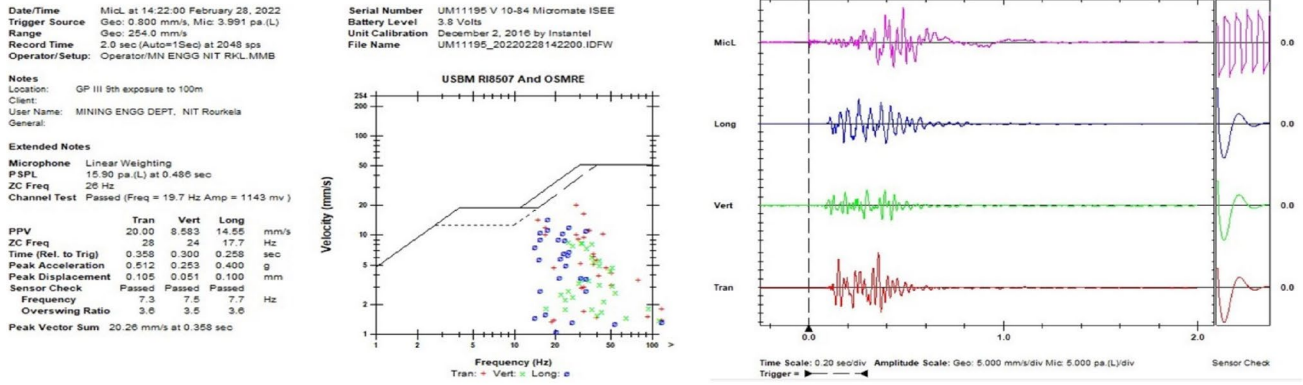


Fig. 6 PPV Readings report exported from Blastware

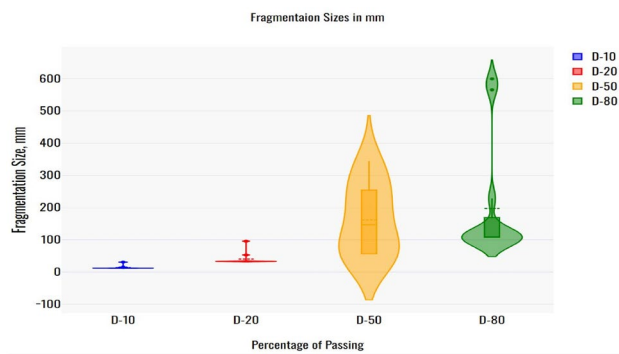


Fig. 7 Various particle sizes produced during blasting

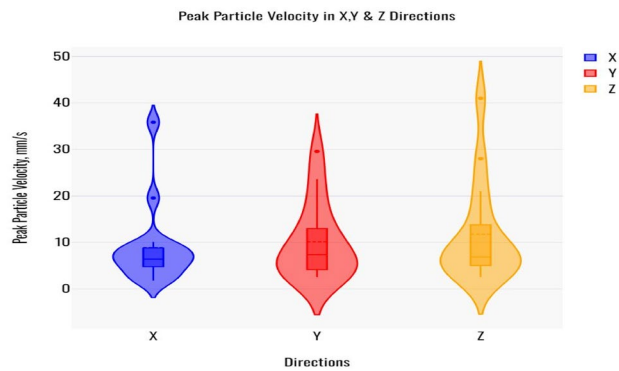


Fig. 8 PPV generated in X, Y and Z directions

Results and Discussions

Influence of Blast Design Parameters on Mean Fragmentation Size

The observed relationship between the mean fragmentation size and the maximum charge per delay reveals a noteworthy trend from Fig. 9. When the explosive charge per delay

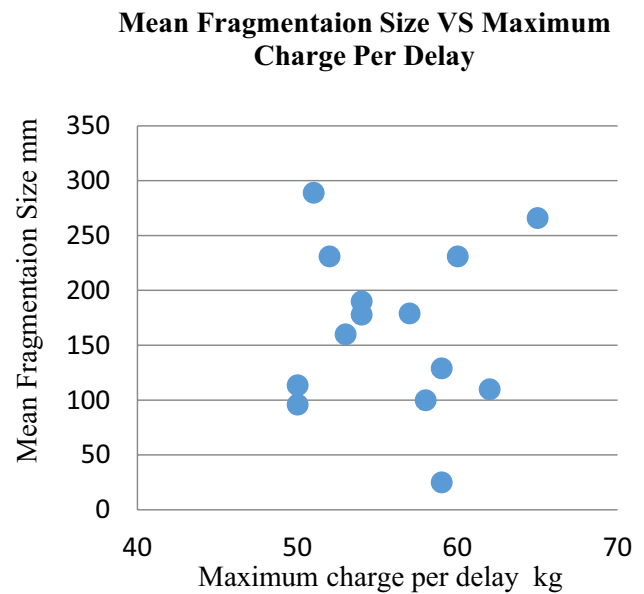


Fig. 9 Influence of MCD on MFS

falls within the range of 55 to 60 kgs, the resultant mean fragmentation size consistently remains below 100 mm. This indicates a critical threshold within this specific charge range, where the explosive energy is optimized for producing finer fragmentation. Conversely, deviations from this optimal charge window—specifically, charges below 55 kgs or above 60 kgs—result in a substantial increase in the mean fragmentation size, surpassing the 100 mm threshold. This suggests that variations in the explosive charge beyond the 55–60 kgs range lead to suboptimal fragmentation characteristics, likely due to inadequate or excessive energy release during the detonation process. The observed increase in mean fragmentation size above 100 mm for charges below 55 kgs implies a diminishing effectiveness of the explosive force, potentially resulting in insufficient breakage of

rock particles. On the other hand, charges exceeding 60 kgs appear to generate excessive energy, leading to larger fragments and, consequently, a higher mean fragmentation size.

As seen in Fig. 10, the 4 m burden demonstrating a propensity for finer fragmentation within the 30 mm to 150 mm ranges. This is due to the interaction of shock waves within the rock mass is crucial; the 4 m burden exhibits better shock wave confinement, resulting in a more controlled breakage process, while longer burdens manifest distinct shock wave interactions leading to larger fragments above 150 mm. Stress wave propagation, influenced by burden length, contributes further to the observed variations in mean fragmentation size. Confinement effects, integral to the control of explosive energy release, show that the 4 m burden strikes an optimal balance, influencing fragmentation within the desired size range. The larger mean fragmentation sizes observed with 3 and 5 m burdens above 150 mm stem from scientific factors such as suboptimal confinement, which allows explosive energy to dissipate over a larger area, insufficient energy distribution for effective breakage within the desired size range, extended stress wave propagation through the rock mass.

As seen Fig. 11, 5 m spacing size excels in achieving a mean fragmentation size of 30 mm due to its optimal energy transfer efficiency. It strikes a balance, avoiding the insufficient energy transfer seen with 3 m and 4 m spacings, as well as the excessive dispersion associated with a 6 m burden. The 5 m size aligns with the critical energy threshold, ensuring effective rock breakage. Geological suitability enhances energy transfer, contributing to the desired fragmentation metric. Additionally, it minimizes wave interference and

Mean Fragmentaion Size VS Bench Height

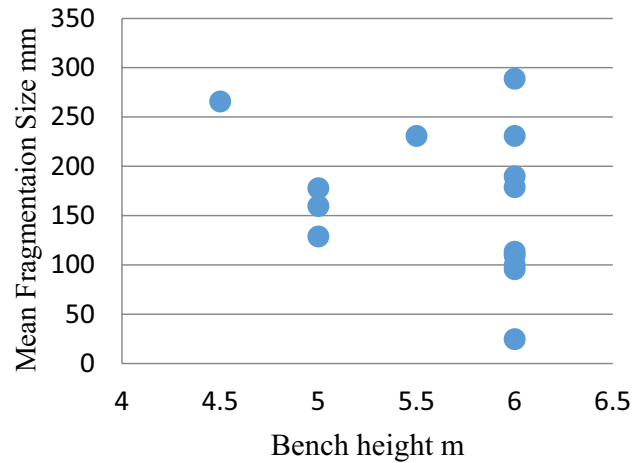


Fig. 11 Influence of Bench height on MFS

confinement issues, resulting in a controlled and finer fragmentation pattern.

The achievement of a 30 mm mean fragmentation size at a 6 m bench height underscores successful fragmentation control, likely due to the balanced coupling of explosive energy with the inherent properties of the rock mass as seen in Fig. 12. The deviation from this optimal state at bench heights of 4, 5, and 7 m, resulting in mean fragmentation sizes exceeding 100 mm, suggests a nonlinear response in fragmentation to changes in bench height. The increase in mean fragmentation size may be attributed to the altered stress wave propagation and energy distribution, leading to larger rock fragments and a departure from the controlled fragmentation observed at the 4, 5 and 7 m bench height.

Mean Fragmentaion Size VS Burden

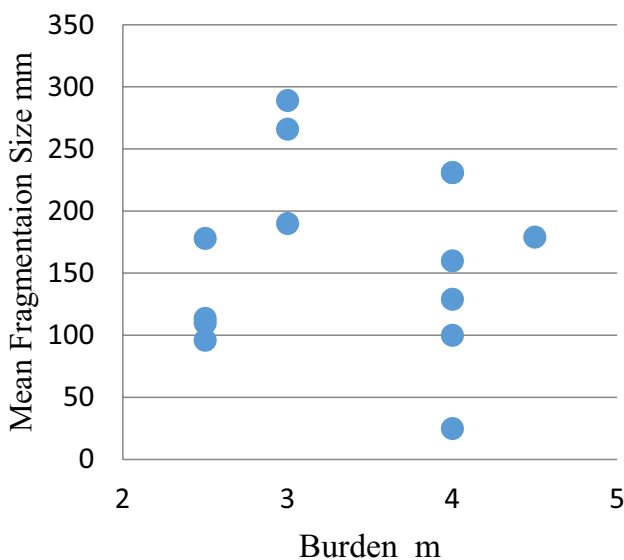


Fig. 10 Influence of burden on MFS

Mean Fragmentaion Size VS Spacing

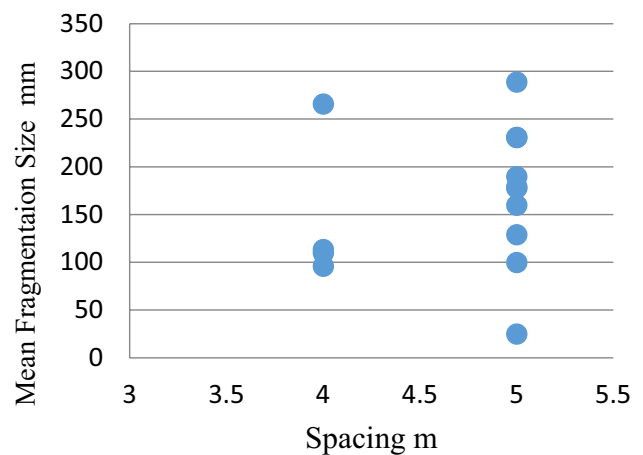


Fig. 12 Influence of spacing on MFS

It is observed from Fig. 13, 3m stemming length, providing optimal confinement for explosive energy and facilitating uniform stress wave propagation, resulting in efficient energy transfer and a controlled, finer fragmentation with a mean size of 30 mm. Shorter stemming lengths (4 m and 5 m) could lead to uneven stress wave release, causing interference and irregular fractures, potentially resulting in larger and less uniform fragment sizes compared to the more controlled release achieved with the 5 m stemming length. The interaction between stemming length and burden size is critical, and a specific burden size may complement the 5 m stemming length, creating an ideal coupling that enhances overall blasting efficiency. Conversely, 3 m and 4 m stemming lengths might not align optimally with the chosen burden, leading to less effective energy transfer and larger fragment sizes.

It is observed from Fig. 14, and mean fragmentation sizes within the 30 to 150 mm range at a powder factor of 2.25 te/kg are indicative of an optimal energy transfer during the blasting process. The specific powder factor appears to foster a balanced interaction between explosive energy and rock properties, resulting in effective fragmentation within the desired size spectrum. Deviations in the powder factor, as noted at 1.5, 2, 2.5, and 3 te/kg, contribute to variations in the mean fragmentation size, particularly exceeding 200 mm. From a blast dynamics perspective, it is due to the lower or higher powder factors disrupt the equilibrium required for controlled rock breakage. Inefficient energy distribution or excessive energy release under these conditions can lead to larger fragmented particles.

Mean Fragmentaion Size VS Stemming

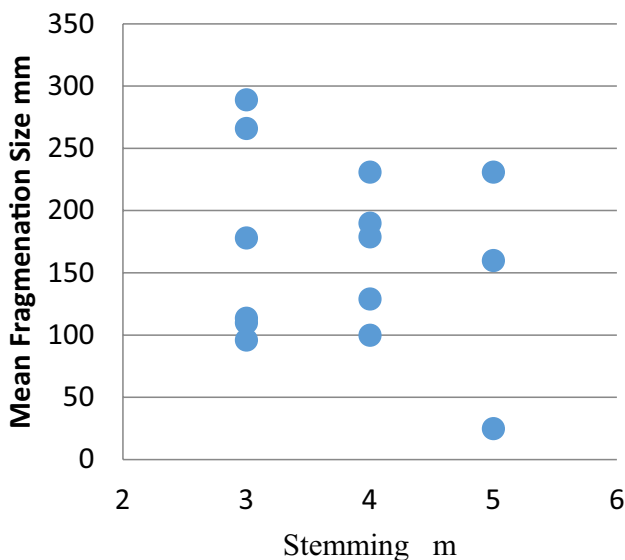


Fig. 13 Influence of stemming length on MFS

Mean Fragmentaion Size vs Powder Factor

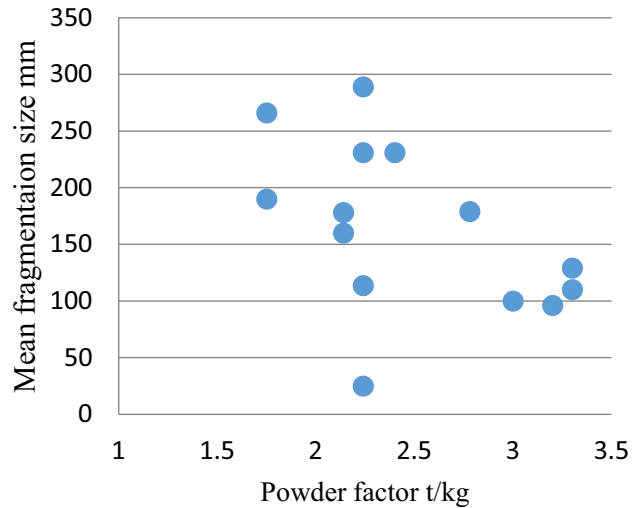


Fig. 14 Influence of Powder factor on MFS

Influence of Blast Design Parameters on Peak Particle Velocity

The amplification of peak particle velocity beyond 10 mm/s with a 6 m spacing, as opposed to the 5 m spacing, can be attributed to the constructive interference of seismic waves, resulting in a more synchronized and cumulative effect that surpasses the damping effects observed at shorter distances as seen in Fig. 15.

From Fig. 16, it is understand that the variation in peak particle velocity within the range of 5–10 mm/s with

Peak Praticle Velocity VS Spacing

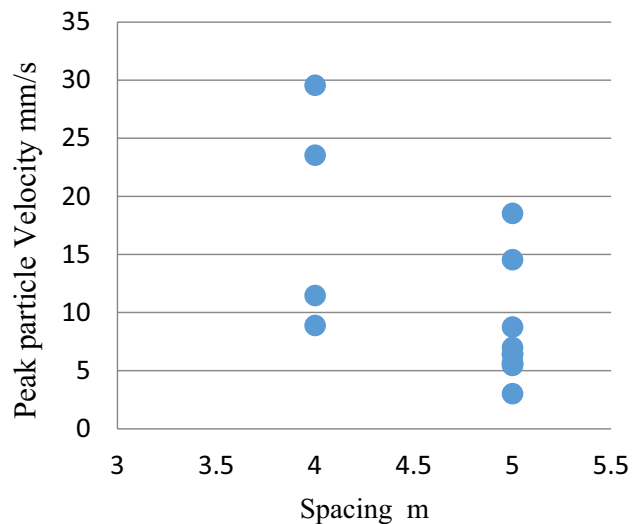


Fig. 15 Influence of spacing on PPV

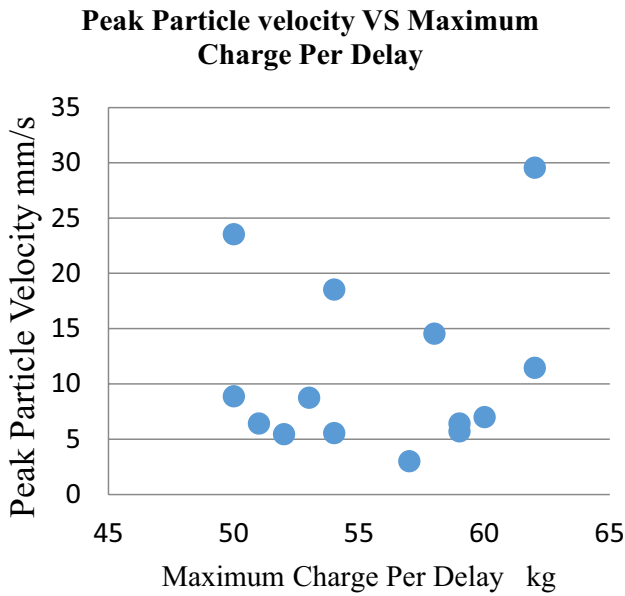


Fig. 16 Influence of MCD on PPV

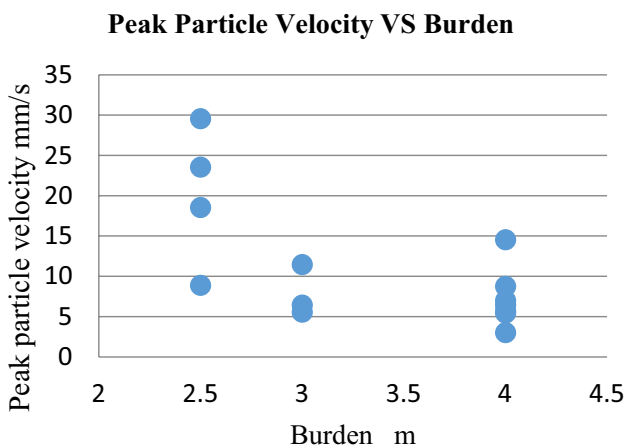


Fig. 17 Influence of burden on PPV

maximum charge per delay is attributed to the nonlinear response of the surrounding rock mass, where charges below 55 kgs exhibit insufficient energy transfer, and charges exceeding 60 kgs result in increased fragmentation and enhanced seismicity, yielding peak particle velocities surpassing 10 mm/s.

The variations in peak particle velocities observed among different burden lengths stem from complex interactions governed by fundamental principles of blasting physics in Fig. 17. The distinctive ability of the 4 m burden to produce lower velocities within the 5 mm/s to 10 mm/s range suggests a unique balance in energy transfer and dissipation mechanisms. In contrast, the consistently higher velocities with 3 and 5 m burdens above 10 mm/s indicate a notable

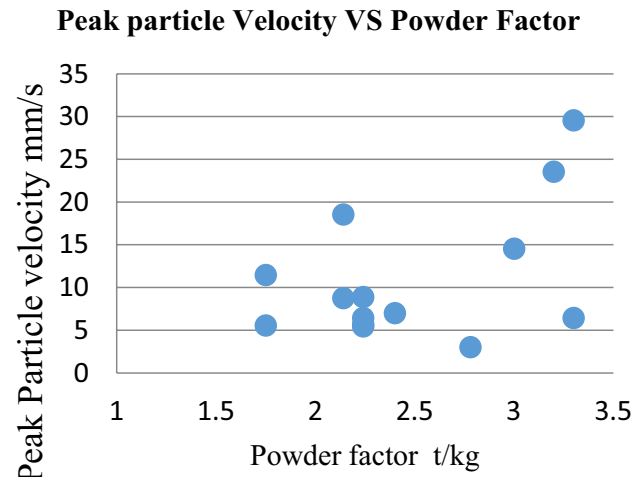


Fig. 18 Influence of Powder factor on PPV

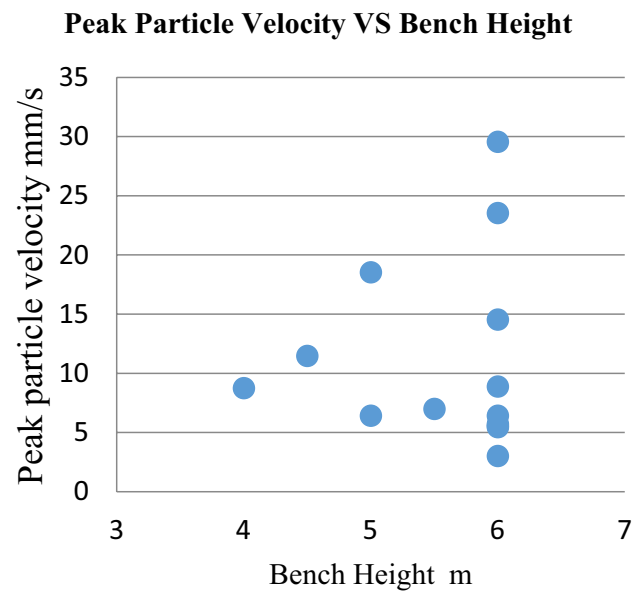


Fig. 19 Influence of bench height on PPV

influence of burden length on shock wave interactions, stress propagation, and geological features.

From Fig. 18, it is observed that increase in peak particle velocity from 5 mm/s to over 10 mm/s with the escalation in powder factor from 2.25 to 3 te/kg within the sequence 0.5, 2, 2.5, 3 can be attributed to the greater explosive energy release at higher powder factors. This elevated energy input enhances the efficiency of stress wave transmission, leading to more effective rock fragmentation processes and consequently resulting in higher peak particle velocities.

It is observed from Fig. 19, the lower peak particle velocity (PPV) within the 5 mm/s to 10 mm/s range at the 6 m bench height can be attributed to intricate interplays of

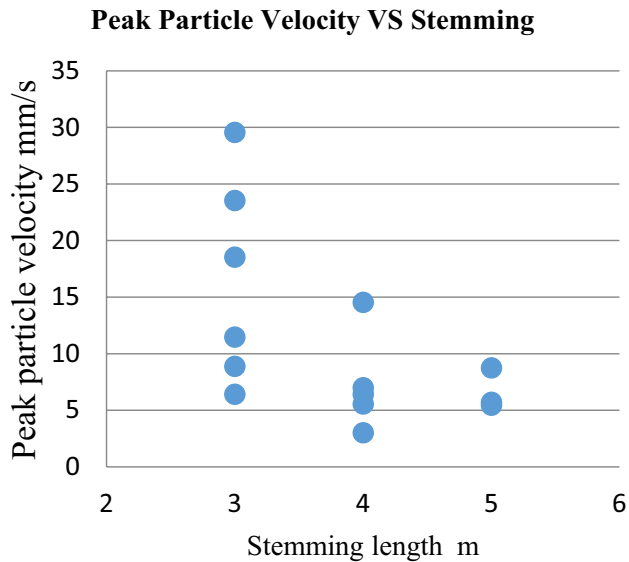


Fig. 20 Influence of stemming length on PPV

energy transfer efficiency, wave attenuation, and confinement effects. The heightened bench allows for a potentially optimized transmission of explosive energy into the rock mass, fostering controlled wave attenuation that minimizes surface vibrations; concurrently, increased confinement may lead to a more regulated release of energy, collectively influencing the dynamic response of the rock and resulting in a subdued PPV within the specified range.

It is seen from Fig. 20; the augmentation in peak particle velocities surpassing 10 mm/s as stemming length extends from 4 to 5 m can be elucidated by the phenomenon of impedance matching, wherein the increased stemming length optimizes the transmission of explosive energy, leading to a resonance effect that amplifies ground motion through the creation of a more coherent wavefront in the rock mass.

Conclusion

An extensive field study was conducted to investigate the influence of various blast design parameters on mean fragmentation size and peak particle velocity, utilizing software and instruments such as WipFrag and Minimate Plus. Numerous variational blasts were executed in the field, involving different blast design parameters such as burden, spacing, bench height, stemming length, powder factor, and maximum charge/delay. The objective was to examine their significant impact on mean fragmentation size and peak particle velocity. The primary findings of the study are as follows:

- It is observed that the explosive charge per delay falls within the range of 55 to 60 kgs, the resultant mean fragmentation size and peak particle velocity are consistently remains below 100 mm and 10 mm/s.
- Similarly, a 4 m burden demonstrating a propensity for finer fragmentation within the 30 mm to 150 mm and low PPV of 10 mm/s.
- A 5 m spacing size excels in achieving successful results in both mean fragmentation size of 30 mm due to its optimal energy transfer efficiency and less peak particle velocity of 10 mm/s.
- The achievement of a 30 mm mean fragmentation size at a 6 m bench height underscores successful fragmentation control and as well PPV seismic drop to 10 mm/s.
- It is observed that the 3 m stemming length provided an optimal confinement for explosive energy and resulted in efficient energy transfer and a controlled, finer fragmentation with a mean size of 30 mm, which also unfolds a significant reduction in PPV to below 10 mm/s.
- The powder factor of 2.25 te/kg are indicative of an optimal energy transfer during the blasting process and produced optimum mean fragmentation sizes within the 30 to 150 mm range and PPV at 10 mm/s.

Funding This research received no external funding.

Data availability The data used to support the findings of this study are available from the corresponding author upon request.

Declarations

Conflicts of interest The authors declare no conflict of interest.

Ethical statement Authors state that the research was conducted according to ethical standards.

References

1. S. Bhandari (1997). Engineering rock blasting operations.
2. T.N. Singh, Artificial neural network approach for prediction and control of ground vibrations in mines. *Min. Technol.* **113**(4), 251–256 (2004)
3. M. Khandelwal, T.N. Singh, Application of an expert system to predict maximum explosive charge used per delay in surface mining. *Rock Mech. Rock Eng.* **46**(6), 1551–1558 (2013)
4. M. Khandelwal, M. Saadat, A dimensional analysis approach to study blastinduced ground vibration. *Rock Mech. Rock Eng.* **48**(2), 727–735 (2015)
5. M. Hajihassani, D. JahedArmaghani, M. Monjezi, E.T. Mohamad, A. Marto, Blast-induced air and ground vibration prediction: a particle swarm optimization-based artificial neural network approach. *Environ. Earth Sci.* **74**(4), 2799–2817 (2015)

6. A.A. Tealeb, M. Sobaih, A.A. Mohamed, K. Abdel-Rahman, Stress level estimation for the ground beneath the 15TH of May city buildings, Helwan, Cairo, Egypt. *Acta Geodaetica et Geophys Hungarica* **38**(4), 429–443 (2003)
7. B. Chateau, J. Peterken, A. Caron, L. Chapdelaine, A. Hagon, C. Druitte, La régionalisation de la radio-télévision de service public, organisation et programmes. *Etudes de Radio-Télévision. Les Cahiers RTB Bruxelles* **32**, 1–123 (1983)
8. N.R. Thote, D.P. Singh, Necessity of blast fragmentation assessment and correlation of rock parameters with blasting performances—a practical approach. *Indian Min. Eng. J.* 19–23 (1997).
9. U.K. Pal, N. Ghosh, Optimization of blast design parameters at SonepurBazari opencast project. *Indian Min. Eng. J.* 41 (2002).
10. D.E. Siskind, Structure response and damage produced by ground vibration from surface mine blasting (Vol. 8507). US Department of the Interior, Bureau of Mines (1980).
11. N Ambraseys, *Rock mechanics in engineering practice*. 1968: Wiley, 111 River Street Hoboken, NJ 07030-6000 USA. p.455
12. N.S. Chandrahas, B.S. Choudhary, M.S. Venkataramayya, Competitive algorithm to balance and predict blasting outcomes using measured field data sets. *Comput. Geosci.* **27**, 1087–1110 (2023). <https://doi.org/10.1007/s10596-023-10254-x>
13. N.S. Chandrahas, B.S. Choudhary, M.V. Teja, M.S. Venkataramayya, N.S.R.K. Prasad, XG boost algorithm to simultaneous prediction of rock fragmentation and induced ground vibration using unique blast data. *Appl. Sci.* **12**(10), 5269 (2022). <https://doi.org/10.3390/app12105269>
14. S. Chandrahas, B.S. Choudhary, N.S.R. Prasad, V. Musunuri, K.K. Rao, An Investigation into the Effect of Rockmass Properties on Mean Fragmentation. *Arch. Min. Sci.* **66**, 561–578 (2021)
15. N.S. Chandrahas, B.S. Choudhary, M.S. Venkataramayya, Firing pattern and spacing burden ratio selection in jointed overburden benches using unmanned aerial vehicle and artificial intelligence based tool. in *Proceedings of the second international conference on emerging trends in engineering (ICETE 2023)*. https://doi.org/10.2991/978-94-6463-252-1_134
16. D. Ramesh, N.S. Chandrahas, M.S. Venkatramayya, M. Naresh, P. Talari, D.U.V.D. Prasad, K.S. Kumar, V.V. Kumar, Effects of spacing-to-burden ratio and joint angle on rock fragmentation: an unmanned aerial vehicle and AI approach in overburden benches. *Acadlore Trans. Geosci.*, 2(3), 155–166. <https://doi.org/10.56578/atg020303> (2023)
17. O.Y. Odeyemi, B.O. Taiwo, O. Alaba, Influence of explosive maximum instantaneous charge on blasting environmental impact. *J. Sustain. Min.* **22**(4), 343 (2023)
18. B.O. Taiwo, Effect of charge load proportion and blast controllable factor design on blast fragment size distribution. *J. Brill. Eng.* **3**(4658), 1 (2022)
19. Z. Zhang, X. Qiu, X. Shi, Z. Luo, H. Chen, C. Zong, Burden effects on rock fragmentation and damage, and stress wave attenuation in cut blasting of large-diameter long-hole stopes. *Rock Mech. Rock Eng.*, 1–19 (2023).
20. B.O. Taiwo, F. Yewuhalashet, O.B. Ogunyemi, V.A. Babatuyi, E.I. Okobe, E.A. Orhu, Quarry slope stability assessment methods with blast induced effect monitoring in Akoko Edo, Nigeria. *Geotech. Geol. Eng.* **41**(4), 2553–3257 (2023)
21. Z. Hong, M. Tao, M. Zhao, J. Zhou, H. Yu, C. Wu, Numerical modelling of rock fragmentation under high in-situ stresses and short-delay blast loading. *Eng. Fract. Mech.* **293**, 109727 (2023)
22. B.O. Taiwo, Y. Fissaha, T. Palangio, A. Palangio, H. Ikeda, N.R. Cheepurupalli, Y. Kawamura, Assessment of charge initiation techniques effect on blast fragmentation and environmental safety: an application of WipFrag software. *Mining* **3**(3), 532–551 (2023)
23. M.S. Venkataramayya, N. Sri Chandrahas, B.S. Choudhary, Identification of most influencing blast design parameters on mean fragmentation size and muckpile by principal component analysis. *Int. J. Innov. Technol. Explor. Eng. Blue Eyes Intelligence Engineering & Sciences Publication*, 201
24. M. Esmaeili, A. Salimi, C. Drebenstedt, M. Abbaszadeh, A. Aghajani Bazzazi, Application of PCA, SVR, and ANFIS for modeling of rock fragmentation. *Arab. J. Geosci.* **8**, 6881–6893 (2014). <https://doi.org/10.1007/s12517-014-1677-3>

Publisher’s Note Springer Nature remains neutral with regard to jurisdictional claims in published maps and institutional affiliations.

Springer Nature or its licensor (e.g. a society or other partner) holds exclusive rights to this article under a publishing agreement with the author(s) or other rightsholder(s); author self-archiving of the accepted manuscript version of this article is solely governed by the terms of such publishing agreement and applicable law.